J Neurophysiol 112: 2076–2091, 2014.
First published August 6, 2014; doi:10.1152/jn.00116.2014.

Encoding of social signals in all three electrosensory pathways of *Eigenmannia virescens*

Anna Stöckl,[1,2] Fabian Sinz,[3,4] Jan Benda,[1,3] and Jan Grewe[1,3]

[1]*Department Biology II, Ludwig-Maximilians-Universität München, Munich, Germany;* [2]*Department of Biology, Lund University, Lund, Sweden;* [3]*Institut für Neurobiologie, Eberhardt Karls Universität Tübingen, Tübingen, Germany; and* [4]*Bernstein Center for Computational Neuroscience, Tübingen, Germany*

Submitted 10 February 2014; accepted in final form 2 August 2014

Stöckl A, Sinz F, Benda J, Grewe J. Encoding of social signals in all three electrosensory pathways of *Eigenmannia virescens*. *J Neurophysiol* 112: 2076–2091, 2014. First published August 6, 2014; doi:10.1152/jn.00116.2014.—Extracting complementary features in parallel pathways is a widely used strategy for a robust representation of sensory signals. Weakly electric fish offer the rare opportunity to study complementary encoding of social signals in all of its electrosensory pathways. Electrosensory information is conveyed in three parallel pathways: two receptor types of the tuberous (active) system and one receptor type of the ampullary (passive) system. Modulations of the fish's own electric field are sensed by these receptors and used in navigation, prey detection, and communication. We studied the neuronal representation of electric communication signals (called chirps) in the ampullary and the two tuberous pathways of *Eigenmannia virescens*. We first characterized different kinds of chirps observed in behavioral experiments. Since *Eigenmannia* chirps simultaneously drive all three types of receptors, we studied their responses in in vivo electrophysiological recordings. Our results demonstrate that different electroreceptor types encode different aspects of the stimuli and each appears best suited to convey information about a certain chirp type. A decoding analysis of single neurons and small populations shows that this specialization leads to a complementary representation of information in the tuberous and ampullary receptors. This suggests that a potential readout mechanism should combine information provided by the parallel processing streams to improve chirp detectability.

communication; decoding; parallel processing; sensory coding; weakly electric fish

PARALLEL PROCESSING OF SENSORY information is a widely used strategy in nervous systems. Parallel channels can result either directly from different types of receptor neurons transducing distinct stimulus features or from neurons further downstream that process a common stimulus in distinct ways. A well-known example for the latter is the mammalian visual system where different neuronal circuits extract color and motion information of a visual stimulus from the same receptors (Wässle 2004; Nassi and Callaway 2009). In other sensory modalities, like somatosensation, parallel processing already starts at the receptor level where different types of receptors extract separate aspects of the sensory input (Bensmaia 2008).

Electroreception in wave-type weakly electric fish is another example for an early separation. Information about the electric field in the fish's vicinity is split into three pathways at the receptor level: the ampullary receptors of the passive electrosensory system detect low-frequency modulations of electric fields, like those created by muscle activity of other animals (Hopkins 1976). T-units and P-units of the tuberous electrosensory system, on the other hand, are tuned to the high frequencies of the electric organ discharge (EOD) generated by the weakly electric fish itself. T-units encode the phase of the EOD and consequently carry precise timing information (Scheich et al. 1973; Hopkins 1976), while P-units spike with a probability that is proportional to the amplitude of the EOD, which itself is modulated by nearby objects, prey, predators, as well as the fields of conspecifics (Bullock and Chichibu 1965; Scheich et al. 1973; Hopkins 1976; Zakon 1986).

Weakly electric fish offer the unique opportunity to experimentally control and electrophysiologically assess the encoding and processing of social signals in the entire electrosensory system. Communication signals (chirps) of *E. virescens*, unlike those of other species of weakly electric fish, contain both low- and high-frequency components that drive all three electroceptors (Hagedorn and Heiligenberg 1985; Metzner and Heiligenberg 1991; Hupé et al. 2008). Studying the neural representation of chirps on the receptor level is therefore important to establish the basis for further studies on electrocommunication in higher brain areas.

The main chirp types described in *E. virescens* are interruptions of the regular EOD, which can last up to 2 s (Hopkins 1974a; Hagedorn and Heiligenberg 1985). During these interruptions, the otherwise balanced EOD develops a DC-offset that gives rise to a low-frequency component stimulating the ampullary receptors (Hopkins 1974a; Metzner and Heiligenberg 1991). Interruptions accompany courtship and mating, are necessary to induce spawning in females (Hagedorn and Heiligenberg 1985), but are also used in aggressive situations by both sexes (Hopkins 1974a). In encounters with conspecifics, amplitude modulations (AM) arise from the interference of the individual EODs. The EOD of each animal will be modulated with a frequency equal to the difference of the individual frequencies. The resulting AM is a beat that constitutes a background signal on which communication signals occur (e.g., Walz et al. 2014). In species in which the EOD frequency exhibits a sexual dimorphism, the nature of the background beat carries information about the type of social encounter (e.g., *Apteronotus* same-sex vs. different-sex encounter, see for example Hupé et al. 2008). In the South-American glass knifefish *E. virescens* (*Sternopygidae*, *Gymnotiformes*) studied here, beats of low frequencies are actively avoided by a change of EOD frequencies in both individuals shifting the beat frequency out of the frequency range used for object detection

Address for reprint requests and other correspondence: J. Grewe, Institut für Neurobiologie, Eberhardt Karls Universität Tübingen, Tübingen, Germany (e-mail: jan.grewe@uni-tuebingen.de).

and navigation. This so-called jamming avoidance response (JAR) exemplifies how the information of two parallel sensory channels, T-units and P-units, of the tuberous system is used to unambiguously determine the difference in EOD frequency and guide the behavior (Heiligenberg 1991).

Chirp encoding in P-units of *Apteronotus leptorhynchus*, a species in which chirps exclusively affect the tuberous system, has been extensively studied in different social encounters, i.e., in different underlying beats (Benda et al. 2005, 2006; Hupé et al. 2008; Marsat and Maler 2010; Vonderschen and Chacron 2011; Walz et al. 2014). In *Eigenmannia*, however, the encoding of EOD interruptions has previously only been assessed in the absence of an EOD of a second fish (Metzner and Heiligenberg 1991). This means that the fish was stimulated solely with its own field and chirps without the beat pattern characteristic of social encounters. Here we investigated the encoding of different communication signals in the presence of a second fish producing chirps. We recorded the neuronal responses in all three types of electroreceptors. We set out by characterizing electrical communication in behavioral experiments. We identify an electric signal that has previously been anecdotally reported as an incomplete interruption, establish it as a chirp in its own right, and describe it in detail. Subsequent in vivo electrophysiological experiments show that this and previously described chirp types elicit qualitatively different responses in P- and T-units while the ampullary receptors encode mainly the occurrence and duration of any type of chirp. In a decoding analysis of single neurons and small populations we demonstrate that the two systems provide complementary information about the different chirp types, which can improve the detectability of these communication signals when combined.

METHODS

All experimental protocols complied with national and European law and were approved by the Ethics Committee of the Ludwig-Maximilians-Universität München (Permit No. 55.2-1-54-2531-135-09). Individuals of *E. virescens* were purchased from commercial fish dealers (Aquarium Glaser, Rodgau, Germany) and kept in colonies of up to 20 fish.

Behavioral Experiments

Fourteen adult fish, 10–21 cm body length, were used for the behavioral experiments. Individual EOD frequencies were between 220 and 550 Hz (383 ± 77 Hz SD, temperature corrected to 26°C). Temperature correction was done applying the average Q_{10} estimated in seven animals (Q_{10} = 1.41 ± 0.11 SD). We did not observe distinct clustering of EOD frequencies, which could have indicated a segregation between males and females, as has been observed in other species of weakly electric fish, such as *Apteronotus* (e.g., Zakon and Dunlap 1999) or *Sternopygus* (e.g. Zakon et al. 1991). Following a phenomenological classification of sexual maturity as used by other authors (e.g., Kramer 1987), all animals were sexually immature, since none of them were gravid with eggs (females, assessed by visual inspection) or in the range of 30-cm body length (males).

Behavioral experiments were conducted in a chirp chamber (Dye 1987; Bastian et al. 2001; Engler and Zupanc 2001; Dunlap and Oliveri 2002) at water temperatures between 24 and 27°C. A fish was placed in a tube covered with a mesh in the middle of a 45-liter tank. Via silver electrodes at the head and the tail the electric field was recorded. A pair of carbon rod electrodes, oriented parallel to the longitudinal axis of the fish, was used for stimulation. The fish was stimulated with sine waves of different frequencies mimicking a conspecific. Stimulus output strength was adjusted to approximately half the fish's EOD amplitude (in the range of 0.5 to 1.5 mV/cm). Difference frequencies (relative to the recorded EOD) of 100, 48, 24, 12, 4, and 0 Hz, both positive and negative, were used.

The head-to-tail-EOD signal was recorded using an extracellular amplifier (EXT 10-2F; npi electronics, Tamm, Germany). Signals were amplified by a factor of 1,000 and band-pass filtered with cutoff frequencies of 0.1 and 30 kHz for the high- and low-pass filter, respectively. Signals were sampled at 30 kHz using a National Instruments data acquisition card (PCI-6295; National Instruments, Austin, TX). Data were analyzed using Matlab (The Mathworks, Natick, MA). Stimulation and recording were controlled by the JAR plugin of the RELACS software package (www.relacs.net). Chirps were detected offline by selecting those frequency excursions that deviated >30 Hz from the baseline EOD frequency (see Fig. 1).

Electrophysiology

Surgery. Twenty-two *E. virescens* (10 to 21 cm) were used for single-unit recordings. Recordings of electroreceptors were made from the anterior part of the lateral line nerve.

Fish were initially anesthetized with 150 mg/l MS-222 (PharmaQ, Fordingbridge, UK) until gill movements ceased and were then respirated with a constant flow of water through a mouth tube, containing 120 mg/l MS-222 during the surgery to sustain anesthesia. The lateral line nerve was exposed dorsal to the operculum. Fish were fixed in the setup with a plastic rod glued to the exposed skull bone. The wounds were locally anesthetized with Lidocainehydrochloride 2% (bela-pharm, Vechta, Germany) before the nerve was exposed. Local anesthesia was renewed every 2 h by careful application of Lidocaine to the skin surrounding the wound.

After surgery, fish were immobilized with 0.05 ml 5 mg/ml tubocurarine (Sigma-Aldrich, Steinheim, Germany) injected into the trunk muscles. Since tubocurarine suppresses all muscular activity, it also suppresses the activity of the electrocytes of the electric organ and thus strongly reduces the EOD of the fish. We therefore mimicked the EOD by a sinusoidal signal provided by a sine-wave generator (Hameg HMF 2525; Hameg Instruments, Mainhausen, Germany) via silver electrodes in the mouth tube and at the tail. The amplitude and frequency of the artificial field were adjusted to the fish's own field as measured before surgery. After surgery, fish were transferred into the recording tank of the setup filled with water from the fish's housing tank not containing MS-222. Respiration was continued without anesthesia. The animals were submerged into the water so that the exposed nerve was just above the water surface. Electroreceptors located on the parts above water surface did not respond to the stimulus and were excluded from analysis. Water temperature was kept at 26°C.

Recording. Action potentials from electroreceptor afferents were recorded intracellularly with sharp borosilicate microelectrodes (GB150F-8P; Science Products, Hofheim, Germany), pulled to a resistance between 20 and 100 MΩ and filled with a 1 M KCl solution. Electrodes were positioned by microdrives (Luigs-Neumann, Ratingen, Germany). As a reference, glass microelectrodes were used. They were placed in the tissue surrounding the nerve, adjusted to the isopotential line of the recording electrode. The potential between the micropipette and the reference electrode was amplified (SEC-05X; npi electronic) and low-pass filtered at 10 kHz. Signals were digitized by a data acquisition board (PCI-6229; National Instruments) at a sampling rate of 20 kHz. Spikes were detected and identified online based on the peak-detection algorithm proposed by Todd and Andrews (1999).

The EOD of the fish was measured between the head and tail via two carbon rod electrodes (11 cm long, 8-mm diameter). The potential at the skin of the fish was recorded by a pair of silver wires, spaced 1 cm apart, which were placed orthogonal to the side of the fish at two-thirds body length. The residual EOD potentials were recorded and monitored with a pair of silver wire electrodes placed in a piece

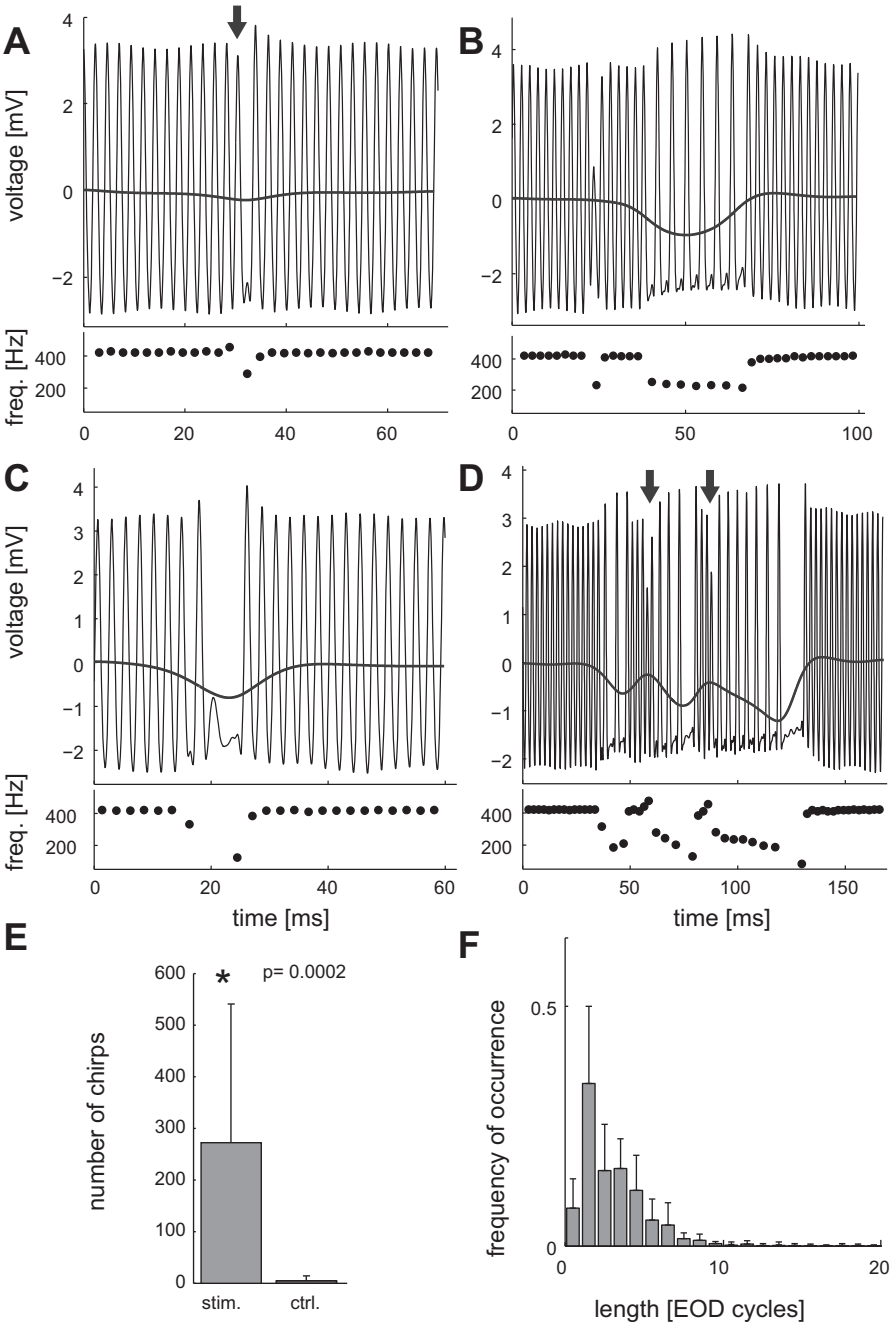

Fig. 1. Characteristics of observed *Eigenmannia* chirps. *A–D*, *top*: voltage traces of electric organ discharges (EODs) containing chirps (light black lines) as well as the low-frequency component estimated by low-pass filtering of the EOD trace (bold black line, filter cutoff at 8 Hz). *A–D*, *bottom*: EOD frequency. Note that recordings originate from different animals and therefore EOD frequencies differ. *A*: single-cycle interruption. *B*: chirp consisting of several repetitions of single-cycle interruptions (type B chirp). *C*: interruption of more than 1 cycle length (type A chirp). *D*: chirp with complex frequency modulations. *E*: number of chirps emitted during 100-s stimulation and control. Significance was evaluated by paired-sample Wilcoxon signed-rank test ($n = 14$, $P = 0.0002$). *F*: distribution of chirp durations measured in EOD cycles averaged across animals ($n = 14$). Error bars indicate SD.

of tube that was put over the tip of the tail. These EOD voltages were amplified by a factor of 1,000 and band-pass filtered between 3 Hz and 1.5 kHz (DPA-2FXM; npi electronics).

Stimuli were attenuated (ATN-01M; npi electronics), isolated from ground (ISO-02V; npi electronics), and delivered by two carbon rod electrodes (30-cm length, 8-mm diameter) placed on either side of the fish parallel to its longitudinal axis. Stimuli were calibrated to evoke defined AM measured close to the fish. Spike and EOD detection, stimulus generation and attenuation, as well as preanalysis of the data were performed online during the experiment within the RELACS software version 0.9.7 using the efish plugin-set (by J. Benda: http://www.relacs.net).

Stimulation. Chirp stimuli consisted of DC playbacks of computer-generated EOD traces containing simplified versions of the different types of EOD interruptions (Fig. 2). Stimuli mimicked conspecific fish with EOD frequencies 24 or 100 Hz above or below the receiving fish. We did not use smaller difference frequencies, since the two-sided JAR of *E. virescens* resulted in difference frequencies of at least 20 Hz, which was in conformity with observations in their natural habitat (Tan et al. 2005). The stimulus intensity was adjusted to AM of 20% contrast (relative to the amplitude of the fish field). The chirp types presented were single-cycle interruptions, multiple repetitions of single-cycle interruptions of 6 and 18 cycles in length (termed type B chirps), as well as prolonged interruptions of 4 and 20 cycles in length (type A chirps).

Every repetition of the stimulus contained 16 chirps, separated by 200 cycles of baseline EOD frequency, and was presented between 15 and 25 times.

Data analysis. We computed continuous firing rates from spike trains by convolution with a Gaussian kernel of a standard deviation of 1 ms. Peristimulus time histograms (PSTH) were obtained by averaging continuous firing rates across trials.

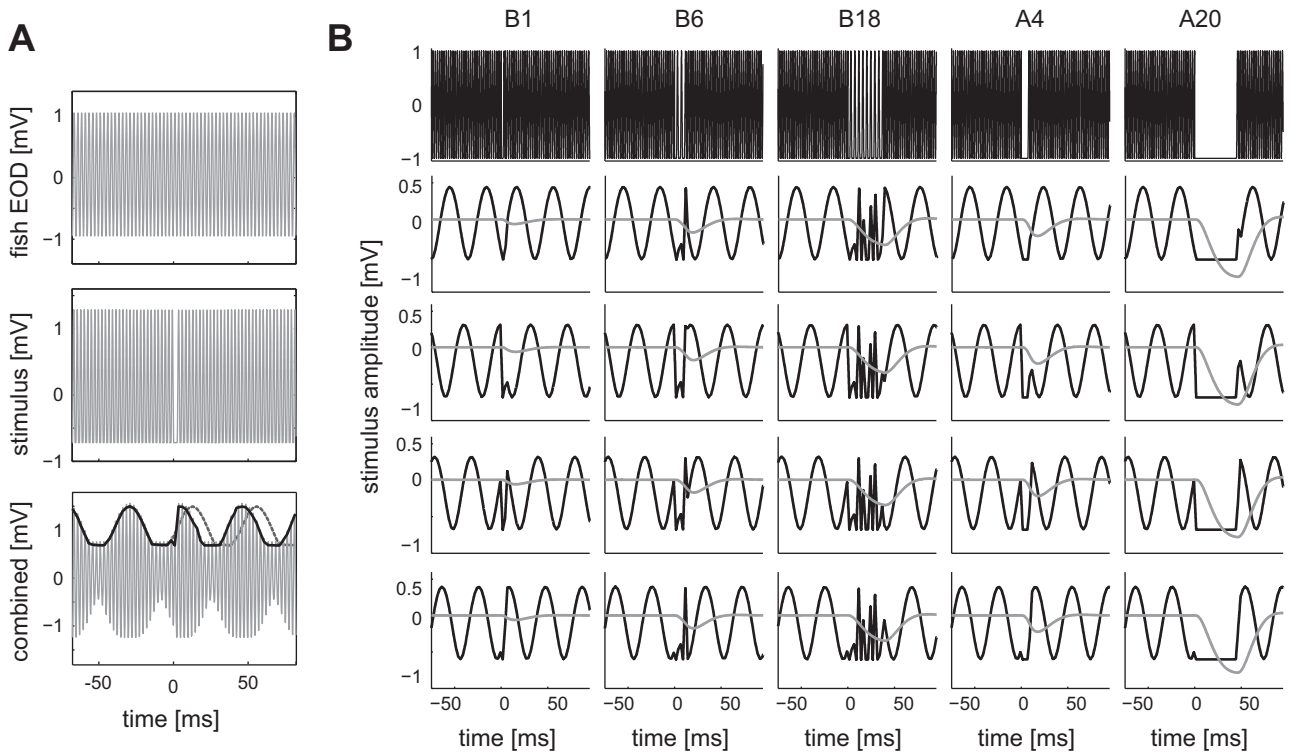

Fig. 2. Different chirp types generated distinct amplitude and low-frequency modulations. *A*: simulated interaction between receiving fish EOD (*top*) and a chirp stimulus (*middle*), resulting in a regular sinusoidal amplitude modulation of the simulated fish EOD, the beat (black line). Chirps interrupted the beat and led to a sudden phase advance (compare black line and dashed gray line illustrating the time course of an uninterrupted beat). *B*: amplitude modulations (black lines) and low-frequency modulations (gray lines) resulting from stimulation with different stimuli. Each column contains a certain chirp stimulus (headings on *top*), and each row illustrates the arising amplitude modulations perceived by the fish at different phase relations to the underlying beat. *1st*, *2nd*, and *3rd columns*: type B chirps. *1st column*: single-cycle interruption (B1 chirp). *2nd* and *3rd columns*: type B chirps of 6 and 18 EOD cycles duration (B6 and B18). *4th* and *5th columns*: type A chirps of 4 and 20 cycles duration (A4 and A20). The low-frequency content of the stimuli was estimated by low-pass filtering (Butterworth low-pass filter, 15-Hz cutoff).

The encoding of chirps was assessed by comparing various response features: the mean firing frequency, the response correlation across trials, and the first derivative of the PSTH.

These features were estimated in three different response sections (see also Fig. 3): *1*) the "chirp response" was estimated in a window of a width that corresponded to the chirp duration plus an additional 2 ms in P-units and 7 ms in ampullary receptors. In P- and T-units, this window was shifted 3 ms relative to chirp onset to account for neuronal delays. In ampullary receptors, the shift amounted to 5 ms. *2*) The "beat response" was calculated by using the same window and the same beat phase as before but in a beat containing no chirp. *3*) Measures derived from these two windows were compared with the "control response" that was calculated from a complete uninterrupted beat cycle for slow beats or several beat cycles at high beat frequencies in P- and T-units. For ampullary receptors the control response was calculated in an 80-ms window preceding chirp onset. Onset responses to chirps in P- and T-units were calculated similarly, but the length of the analysis windows for the chirp response and beat response was shortened to one EOD cycle.

The phase relation between the chirps and the beat was extracted during offline analysis. The phase of chirp onset (ϕ) was calculated as

$$\phi = 2\pi \frac{t_S - t_{EOD}}{T_{EOD}} \quad (1)$$

where t_{EOD} was the time of the last EOD cycle before chirp onset, t_S was the time of chirp onset, and T_{EOD} the period of the EOD. We discriminated 10 chirp phases, sorted the responses of P-and T-units according to their onset phase and analyzed them separately. Ten chirp phases provided fine enough binning to ensure that only chirps occurring in very similar phases would be analyzed together, thus minimizing the effect of averaging out response characteristics across phases. Ampullary responses were pooled across phases since ampullary receptors are not driven by the beat.

We computed the mean firing rate in P-units and ampullary receptors. The mean spike train correlation and absolute derivative of the PSTH were only estimated in P-units. The mean firing rate was quantified as the average of the continuous spike train in the respective window and averaged over trials. The spike train correlation was quantified according to Benda et al. (2006) as the correlation coefficient

$$r_{ij} = \frac{\langle (s_i - \langle s_i \rangle_t)(s_j - \langle s_j \rangle_t) \rangle_t}{\sqrt{\langle (s_j - \langle s_j \rangle_t)^2 \rangle_t} \sqrt{\langle (s_j - \langle s_j \rangle_t)^2 \rangle_t}} \quad (2)$$

of all possible pairs, s_i and s_j, of spike trains evoked by repeated stimulation and convolved with a Gaussian. Brackets $\langle \cdot \rangle_t$ denote averages over time. The mean spike train correlation was obtained by averaging r_{ij} over all pairs of spike trains.

In T-units, the interspike intervals (ISIs) were used for the analysis of chirp responses. A continuous representation of ISIs was obtained by convolving ISIs with a Gaussian kernel with a standard deviation of 1 ms. Mean ISI and correlation of ISIs were computed as discussed for the firing rate of P-units.

Response duration in ampullary receptors was calculated as the time the firing rate exceeded baseline firing rate plus four times the standard deviation of the average baseline firing rate. This was adjusted by visual inspection to give the closest match with the chirp duration.

Decoding analysis. All decoding analyses were based on the SciPy (http://www.scipy.org), sklearn, and matplotlib packages of python (Pedregosa et al. 2011; Hunter 2007).

For the decoding analysis we extracted segments from the neuronal responses that either contained a chirp (chirp responses) or that were randomly placed in the interchirp interval, i.e., when the simulated second fish was present but did not chirp (baseline responses). The decoding task was to discriminate a chirp from baseline response. Our analysis was performed for the 24-Hz beat condition. Since the EOD frequencies of the recorded fish varied between 280 and 510 Hz, the applied chirp stimuli had to vary accordingly. The width of the data

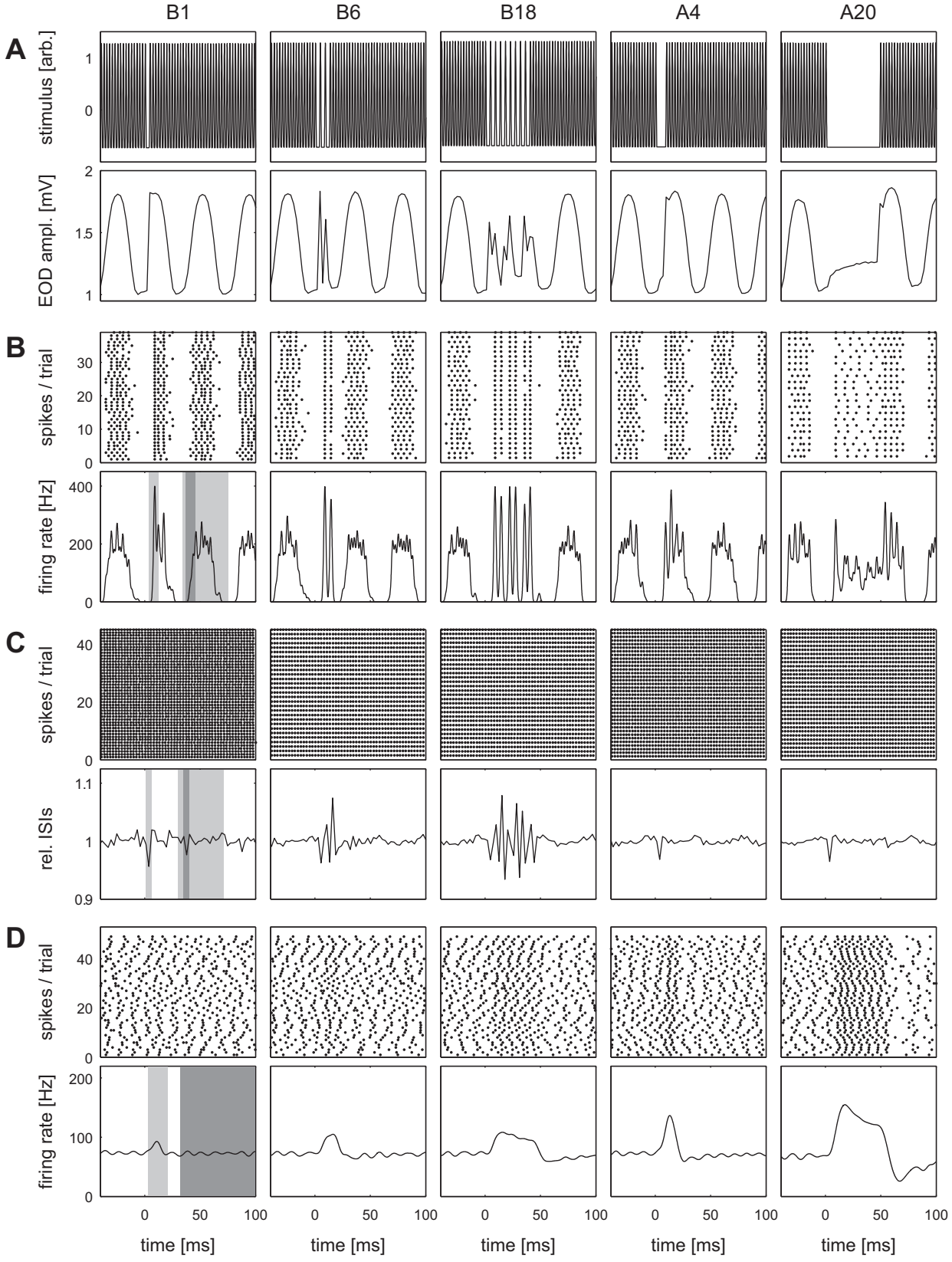

segment was hence based on EOD cycles instead of fixed temporal durations. Data segments of duration D ∈ 5, 10, 20, 25, 30 EOD cycles were used.

We simulated small populations of receptor neurons by combining responses of different neurons recorded in the same animal to the same chirp type. Therefore, the number of trials for one particular chirp type was equal to the minimal number of trials for that condition for all neurons participating in the population. If more responses were recorded from one neuron, a random selection was dropped.

Support vector machines were used (SVMs; Boser et al. 1992; Cortes and Vapnik 1995) to classify the receptor responses to a particular chirp type against its baseline activity. SVMs learn decision rules of the form

$$\hat{y} = \text{sign}\left[\sum_{i=1}^{m} \alpha_i k(x_i, x) + b\right] \tag{3}$$

from labeled data sets $\{(y_i,x_i)\}_{i=1}^m$, where $y_i \in \{-1,1\}$ is the label that indicates whether a trial x_i is a chirp or a baseline response. $\hat{y}$ is the label that the SVM predicts for the trial x. The function k is a positive semidefinite Mercer kernel that corresponds to a dot-product $k(x,x_i) = \langle \phi(x), \phi(x_i) \rangle$ between two feature vectors $\phi(x)$ and $\phi(x_i)$ computed from the data points x and x_i, respectively (Schölkopf and Smola 2002). Using the bilinearity of the dot product, one can see that the inner part of *Eq. 3* is a linear function of the feature vector $\phi(x)$

$$\begin{aligned}\sum_{i=1}^{m} \alpha_i k(x_i, x) + b &= \left\langle \sum_{i=1}^{m} \alpha_i \phi(x_i), \phi(x) \right\rangle + b = \left\langle w, \phi(x) \right\rangle + b \\ \text{for } w &= \sum_{i=1}^{m} \alpha_i \phi(x_i).\end{aligned} \tag{4}$$

In all analyses for single neurons, we use

$$k(x_1, x_2) = \int_0^T (x_1 * h)(t)(x_2 * h)(t)\,dt, \tag{5}$$

where $x_\ell * h$ denotes the convolution of a filter kernel h with a spike train $x_\ell = \sum_i \delta\left(t - t_i^{(\ell)}\right)$. We use a one-sided exponential filter $h(t) = [t]_+ \cdot \exp\left(-t/\tau\right)$ with $\tau = 1$ ms to simulate the input to a pyramidal cell postsynaptic to the receptors. *Equation 5* can be computed more efficiently by solving the integral analytically resulting in (Park et al. 2013)

$$\begin{aligned}k(x_1, x_2) &= \int_0^T (x_1 * h)(t)(x_2 * h)(t)\,dt \\ &= \frac{\tau}{2} \sum_{i,j} \exp\left(-\frac{\left|t_i^{(1)} - t_j^{(2)}\right|}{\tau}\right),\end{aligned}$$

where i and j run over the number of spikes in x_1 and x_2, respectively. Note that by putting the definition of the kernel in *Eq. 5* into *Eq. 4* and using $\phi(x_i) = (h * x_i)(t)$, the decision function is given by

$$\hat{y} = \text{sign}\left[\sum_{i=1}^{m} \alpha_i k(x_i, x) + b\right] = \text{sign}\left[\int_0^T w(t) \cdot (x * h)(t)\,dt + b\right]$$
$$\text{with } w(t) = \sum_{i=1}^{m} \alpha_i \phi(x_i).$$

This means that the decision function is equivalent to integrating a weighting function w against the spike train x convolved with h. The weighting function $w(t)$ can be plotted to find epochs within the spike train that strongly influence the decision of the classifier (see Fig. 9).

For analyzing the prediction performance of populations, we generated a kernel on the population by summing the kernel values of the constituent neurons. For example, assume we have trials from a population consisting of an ampullary (a), a P-unit (p), and a T-unit (t), the kernel between the first and the second trial from that population was computed as

$$\begin{aligned}&k\left(\left\{x_1^{(a)}, x_1^{(p)}, x_1^{(t)}\right\}, \left\{x_2^{(a)}, x_2^{(p)}, x_2^{(t)}\right\}\right) = \\ &k\left(x_1^{(a)}, x_2^{(a)}\right) + k\left(x_1^{(p)}, x_2^{(p)}\right) + k\left(x_1^{(t)}, x_2^{(t)}\right).\end{aligned}$$

This is equivalent to stacking the feature vectors $\phi(x^{(a)})$, $\phi(x^{(p)})$, and $\phi(x^{(t)})$ to obtain a combined feature vector $\phi(\{x^{(a)}, x^{(p)}, x^{(t)}\})$.

To find the parameters α_i,b for a given dataset, we used the SVM implementation included in the Python package sklearn (Pedregosa et al. 2011). Before training, all data points $\phi(x_i)$ were centered on the mean over the training set. This can be done implicitly on the matrix $\mathbf{K} = [k(x_i,x_j)]_{ij}$, $1 \le i,j \le m$ of pairwise kernel values (Schölkopf and Smola 2002). To decrease computational time, we limited the number of baseline trials to 1,000. The number of chirp trials was typically ~300.

The training stage of the SVM includes a regularization parameter $C \in \mathbb{R}_+$ that trades off complexity of the decision function (4) against classification accuracy on the training set (Schölkopf and Smola 2002). We determined the best value for C by running a fivefold stratified cross validation for each $C \in \{10^{-4}, 10^{-3.5}, ..., 10^{3}\}$ choosing the value with the best average accuracy over folds (Duda et al. 2000). Since the number of trials for the baseline activity and chirp responses were usually not the same, we used additional weighting factors provided by the implementation of the SVM that make a misclassification of a data point more costly if it comes from the underrepresented class (Pedregosa et al. 2011).

To measure how well chirps can be classified against baseline, we used mutual information (Cover and Thomas 2006)

$$I\left[\hat{Y} : Y\right] = \text{E}_{Y,\hat{Y}}\left[\log_2 \frac{P\left(Y, \hat{Y}\right)}{P(Y)P\left(\hat{Y}\right)}\right] \tag{6}$$

between the true Y and the predicted label $\hat{Y}$, which yields a lower bound on the information that the neural response provides about the presence or absence of a chirp (Quian Quiroga and Panzeri 2009). The maximally possible value of $I[\hat{Y} : Y]$ if given by $I[Y : Y] = -\left\langle \log_2 P(y) \right\rangle_Y \le 1$ bit and, thereby, depends on the percentages of the particular label in the dataset. Since these percentages can vary depending on how many trials were recorded from that particular neuron, we normalize the mutual information by its maximum $I[\hat{Y} : Y] = I[Y : Y]$ and report this value in percent to make the decoding performance comparable between neurons and subjects.

To estimate *Eq. 6* from a finite number of data points, we first estimated the joint distribution $P(\hat{Y} : Y)$ via the relative frequency of the different value combinations of $(y,\hat{y}) \in \{-1,1\}^2$ on a stratified test set consisting of 20% of the trials withheld from the SVM during the training stage. Afterwards we obtained $P(Y)$ and $P(\hat{Y})$ via marginalization and plugged the resulting distributions into *Eq. 6*. To assess the

Fig. 3. All 3 types of electroreceptors respond to all chirp types. *A*: stimuli mimicked the EOD of a chirping fish (*top row*) that resulted in an amplitude modulation of the EOD of the receiving fish (stimuli were calibrated to modulate the EOD amplitude by 20%). *B*: P-unit responses with spike rasters in the *top row*, and peristimulus time histogram (PSTH) in the *bottom row*, respectively. Shaded areas at *left* mark the analysis windows. From *left* to *right*: chirp response (gray area, aligned with the chirp), beat response (dark gray area, same length and phase relation with the beat as the chirp response, but placed in an uninterrupted beat), and control response (gray area, covering a full beat cycle). *C*: responses and analysis windows of T-units (see *B* for details). Note that the *bottom row* shows the interspike intervals (ISI) relative to the average ISI recorded at rest instead of the firing rate. *D*: responses of ampullary receptors. Here, only the chirp response (grey) and control response (dark grey) were analyzed.

variability of the mutual information estimates, we resampled training and test sets 10 times and repeated the SVM training procedure along with the subsequent mutual information estimation.

RESULTS

Frequency Modulations in Response to Mimicks of Conspecifics

We characterized the electric communication of *E. virescens* in behavioral experiments. Animals were stimulated with sinusoidal electrical signals mimicking conspecifics with a range of EOD frequencies. All animals performed a two-sided JAR in which they increased their EOD frequency upon negative difference frequencies and vice versa as described in the literature (Watanabe and Takeda 1963; Bullock et al. 1972; Heiligenberg 1980, 1991), indicating that they responded to stimulation as they would do to conspecifics. All tested animals showed a JAR, but individual differences in the response strength could be observed.

In 16 out of 60 chirp-chamber experiments, the tested individuals produced brief frequency modulations. The most common ones are exemplified in Fig. 1; 73.7% of these frequency excursions were decreases of the EOD frequency, i.e., interruptions. Since they were almost exclusively produced upon stimulation (Fig. 1*E*), we interpreted them as communication signals. The chirps consisted of EOD interruptions as well as single cycles of increased frequency (arrows in Fig. 1, *A* and *E*). The most common modulations observed were EOD interruptions of one cycle length, which we termed single-cycle interruptions (Fig. 1*A*). Interruptions of single-cycle length occurring in multiple repetitions (effectively decreasing the EOD frequency to half its baseline value, Fig. 1*B*) were frequently observed as well. We refer to these patterns as type B chirps to distinguish them from the long-lasting complete interruptions that are not interspersed by EODs and have previously been described (Hopkins 1974b; Hagedorn and Heiligenberg 1985) that we call "type A" chirps. In our experiments, we observed a few interruptions lasting longer than one EOD cycle (Fig. 1*C*) but never as long as previously described type A chirps (Fig. 1*F*). In many cases, chirps were more complex combinations of the three described patterns, often interrupted by a few baseline EOD cycles (Fig. 1*D*). During all types of interruptions, the negative offset of the EOD remained, while the counterbalancing positive peaks were missing, thus giving rise to low-frequency components in the signal (Fig. 1).

Effect of Chirps on the Electric Field of a Receiving Fish

To characterize how chirps are encoded by the three types of electroreceptors, we performed in vivo electrophysiological experiments in which we stimulated the fish with simplified reconstructions of chirps. We investigated which features of the observed frequency modulations are relevant for the sensory perception of communication signals and whether chirps would be discriminable in the sensory domain.

Reconstructions of type B chirps observed in the behavioral experiments, as well as type A chirps described in the literature (Hopkins 1974a; Hagedorn and Heiligenberg 1985) (Fig. 2), were presented to the animal. These chirps were embedded in mimics of a second fish's EOD that led to beat frequencies of 24 and 100 Hz. During the interchirp intervals, the receiving fish was thus stimulated with the continuous amplitude modulation caused by the foreign EOD. Chirps interrupt this continuous beat (Fig. 2*A*), which led to changes in the beat and the low-frequency content of the stimulus. The beat is phase shifted by the chirps as described before for other species of weakly electric fish (Benda et al. 2005, 2006). The chirp-induced phase shifts led to EOD AM (rising and falling flanks) that were steeper than those during the beat. This is particularly true if the interruption occurred in early phases of the rising or falling flanks of the beat cycle. The beat phase at which the chirps occurred heavily influenced the amplitude modulation for short interruptions (*1st*, *2nd*, and *4th columns* in Fig. 2*B*). For long interruptions, the phase relation was not relevant (*3rd* and *5th columns* in Fig. 2*B*). Cessation of EODs during chirps further induced low-frequency shifts of the stimulus that drove ampullary receptors. In contrast to P-units and T-units, however, these are generally independent of the beat phase in which the chirp occurs (grey lines in Fig. 2*B*).

In the following paragraphs we show the responses of P-units, T-units, and ampullary receptors to the different chirp stimuli.

P-Units Respond to AM During Chirps with a Change in Firing Rate and Synchrony

P-unit electroreceptors encode AM of the fish's own EOD in the modulation of their firing rate: the firing rate increases upon amplitude increases and vice versa. Correspondingly, the firing rate of P-units was sinusoidally modulated in response to stimulation with beats only (Fig. 3*B*). Chirps that lead to increases in EOD amplitude induced a firing rate increase exceeding the maximum firing rate during the beat. If the chirp led to decreases in EOD amplitude, the firing rate also decreased (Fig. 3*B*). In addition, chirps also influenced the synchrony of P-unit responses. Sudden changes in amplitude modulation led to high degrees of synchrony across multiple repetitions of the same stimulus, which can be regarded as a proxy for the responses of multiple neurons in the receptor population (Benda et al. 2005). As shown in Fig. 2, the phase relation between chirp and underlying beat strongly influenced the EOD amplitude modulation; hence, subsequent analysis was performed for each phase relation separately.

Different response features were evaluated and compared between the chirp (*chirp response*), the corresponding beat phase (*beat response*), as well as the response to a complete beat cycle (*control response*), to quantitatively analyze the effects of chirps on the P-units.

During single-cycle interruptions in a 24-Hz beat, the mean firing rate was sinusoidally modulated around the average firing rate across chirp phases (Fig. 4*A*, *1st column*). It was shifted with respect to the firing rate during the beat in most phases. The response synchrony, evaluated as the correlation across trials, was higher during the chirp response than during beat and control responses in many chirp phases (Fig. 4*A*, *middle*). Moreover, the firing rate of P-units changed more rapidly in response to chirps than it did in response to the beat,

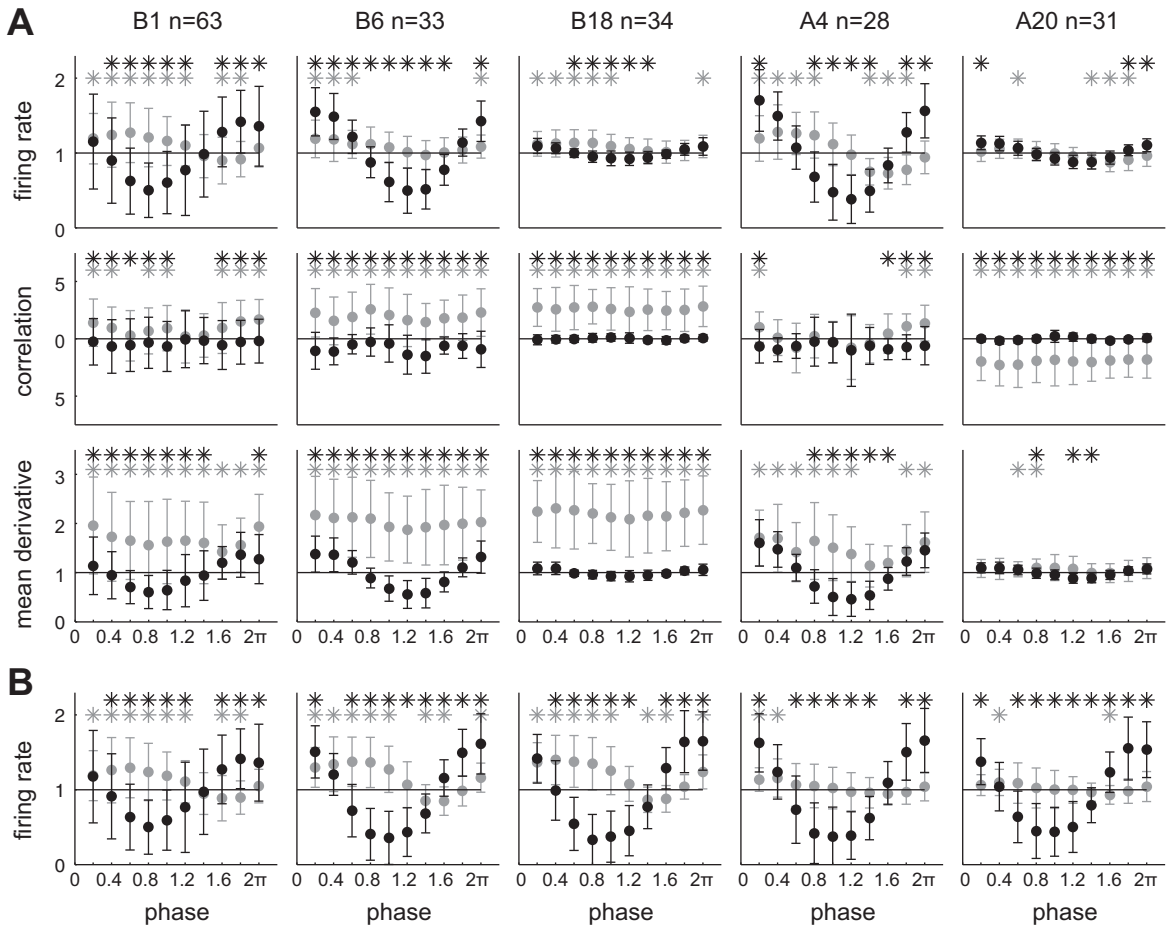

Fig. 4. Distinct response patterns to different chirp types in a 24-Hz beat in P-units. Averaged responses of P-units to the different chirp types (see Fig. 2) in a 24-Hz beat. *A*: effects of chirps on the average firing rate, the response correlation, and the derivative of the PSTH were analyzed for 10 different phase relations between chirp and beat. *B*: firing rate was analyzed for the onset (first EOD cycle) of the chirp. Error bars denote SD. Measures in the chirp response (gray dots) and beat response (black dots) were normalized to the control response (horizontal line, compare Fig. 3). Asterisks indicate a $P < 0.01$ in a Wilcoxon signed-rank test between chirp and beat response (black asterisks) as well as chirp and control response (gray asterisks).

as evaluated by the derivative of the firing rate (Fig. 4*A*, *bottom*).

With an increasing duration of type B chirps, synchrony in the chirp response increased and was substantially higher than both the beat- and control response across all phases (Fig. 4*A*, *2nd* and *3rd columns*). The derivatives of the firing rate increased significantly above beat and control values as well. For long type B chirps, the firing rate did not differ from beat and control values, because P-units responded with alternating increases and decreases in firing rate, averaging out over the course of the chirp.

Type A chirps had similar effects on the firing rate as type B chirps (Fig. 4*A*, *4th* and *5th columns*). The longer the interruption, the less the firing rate modulation across phases and the smaller the difference between chirp response and beat response, as well as the control response.

In contrast to type B chirps that increased response synchrony, type A interruptions reduced synchrony significantly. This effect was stronger the longer the interruption lasted (compare Fig. 4*A*, *middle*).

Both upon long type A and type B chirps, P-units responded to the modulation generated at the onset (Fig. 4*B*) and offset of the chirp with a modulation in firing rate similar to single cycle interruptions, because at onset and offset all chirp types generated the same abrupt changes in EOD amplitude.

Frequency and Sign of the Beat Did Not Alter P-Unit Responses to Chirps Qualitatively

Chirps embedded in a 100-Hz beat led to qualitatively similar, yet weaker, responses compared with 24-Hz beats (Fig. 5). Because the AM of the fast beat alone were already quite effective in driving the neurons to their firing rate limits, changes caused by the chirps had less impact. The spike-train correlation and the PSTH derivatives upon long type A chirps decreased much stronger at 100-Hz than at 24-Hz beats, because the firing was stronger correlated during fast than during slow beats and therefore interruptions had a stronger decorrelating effect. In fast beats, the mean firing rate upon long type A and type B chirps was not modulated with respect to the beat, which was similar to slow beats.

The quality of P-unit responses to chirps was independent of the sign of the beat. Chirps embedded in a 24-Hz beat of negative difference frequencies (i.e., the receiving fish has a higher EOD frequency than the fish producing the chirps) led to qualitatively very similar responses as chirps in positive beats of the same frequency.

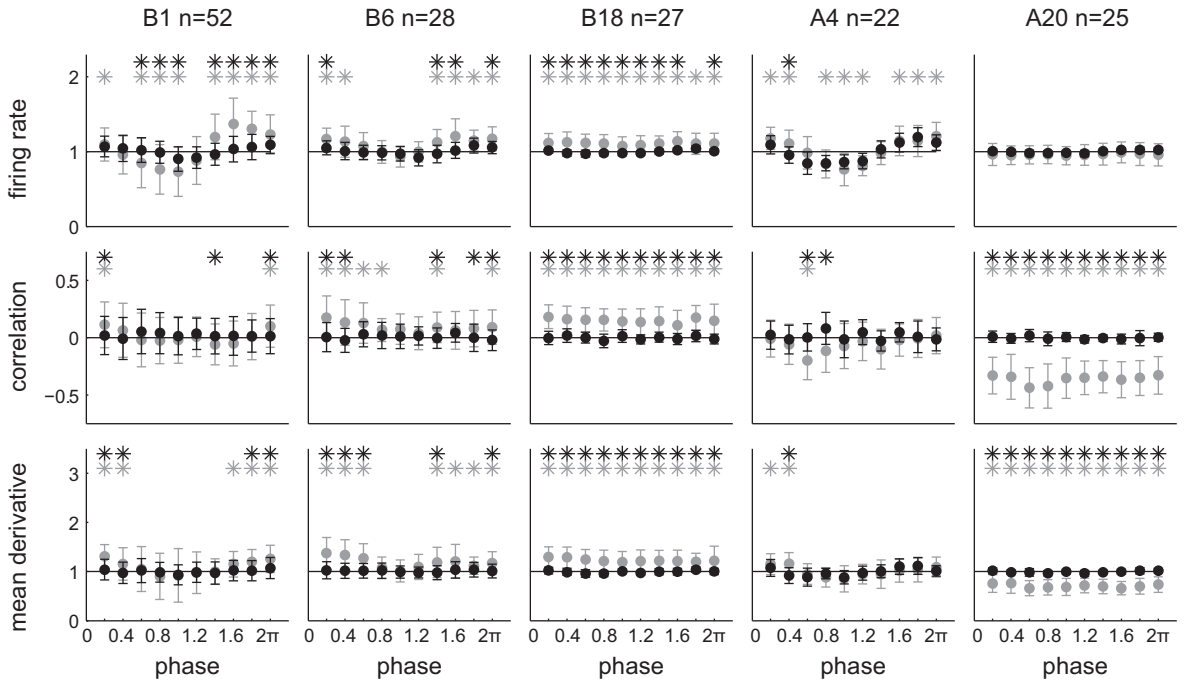

Fig. 5. Similar P-unit response patterns to chirps in fast beats. Similar experiment and analysis as in Fig. 4, but chirps were now embedded in a 100-Hz beat.

Heterogenous P-Unit Responses

Although general response patterns could be extracted for all P-units, there was a substantial amount of heterogeneity in the responses (see error bars in Figs. 4 and 5), due to the heterogeneity of P-units in their baseline firing rate. P-units with a very high baseline firing rate close to the EOD frequency were not able to increase their firing frequency substantially upon amplitude upstrokes caused by chirps; thus their response was much more pronounced to chirps causing downstrokes of the EOD amplitude. The opposite was true for P-units with very low baseline firing rates (shown in Fig. 6 for 2 example cells).

T-Units Respond to Chirps with Changes in Spike Timing

T-units are the second receptor type of the tuberous electrosensory system that are driven by the fish's own EOD and fire one spike in a phase-locked manner to every EOD cycle. Thus, encoding of chirps in the firing rate is not possible. However, it has been reported that T-units encode phase modulation during beats in their spike timing (Bastian and Heiligenberg 1980; Rose and Heiligenberg 1986; Lytton 1991; Fortune et al. 2006). Therefore, we analyzed the ISIs of T-units as a measure of spike timing, as well as the correlation of ISIs across stimulus repetitions.

T-units showed modulations of their ISIs in response to chirps (Fig. 3*A*). Upon single-cycle interruptions, their ISIs decreased if the interruption generated a rising flank in amplitude and increased if it generated a falling flank (Fig. 3*C*). The positive and negative deflections of the mean ISI were larger during chirps than during the beat.

A pattern very similar to P-units emerged when analyzing T-unit ISIs and their correlation across trials for the different chirp types: for single-cycle interruptions, the ISIs were sinusoidally modulated around the control across phases and shifted in phase with respect to the beat response (Fig. 3*B*). The correlation of ISIs across trials was higher than the correlation during the beat in a few phases only. With increasing length of type B interruptions, the ISI modulations relative to the beat decreased, but the correlation in ISIs between trials increased. Upon longer type A chirps both the ISI modulations and the correlation across trials were not different from the beat values (Fig. 7*A*).

Similar to P-units, T-units also modulated their ISIs at the beginning and end of a chirp irrespective of chirp type (Fig. 7*B*).

Ampullary Receptors Respond to Low-Frequency Components of All Chirp Types

Ampullary receptors belong to the passive electrosensory system and are tuned to low-frequency modulations in the electric field. When the EODs of two fish interact in a communication context, the receiving fish's EOD is amplitude modulated (compare Fig. 2*A*). Ampullary receptors are not driven by this AM (Fig. 3*D*, period before chirp onset). During the chirp, however, when the chirping fish ceased generating the positive deflections of its EOD, the negative DC component prevails and induces low-frequency signals (solid black lines in Fig. 1 and gray lines in Fig. 2*B*), which drive the ampullary receptors. The neurons responded to the chirps with an increase in firing rate (Fig. 3*D*).

Since ampullary receptors are not driven by the fish's own EOD and its amplitude modulation, the phase relation of chirp and beat is not relevant and data were pooled across phases. Ampullary receptors encoded the duration of the chirp with the duration of their response (Fig. 8*A*). With increasing duration of the interruption, the difference between chirp response and control response increased in a linear way (Fig. 8*B*). However, type A interruptions triggered larger ampullary responses than type B interruptions of similar length, corresponding to their different low-

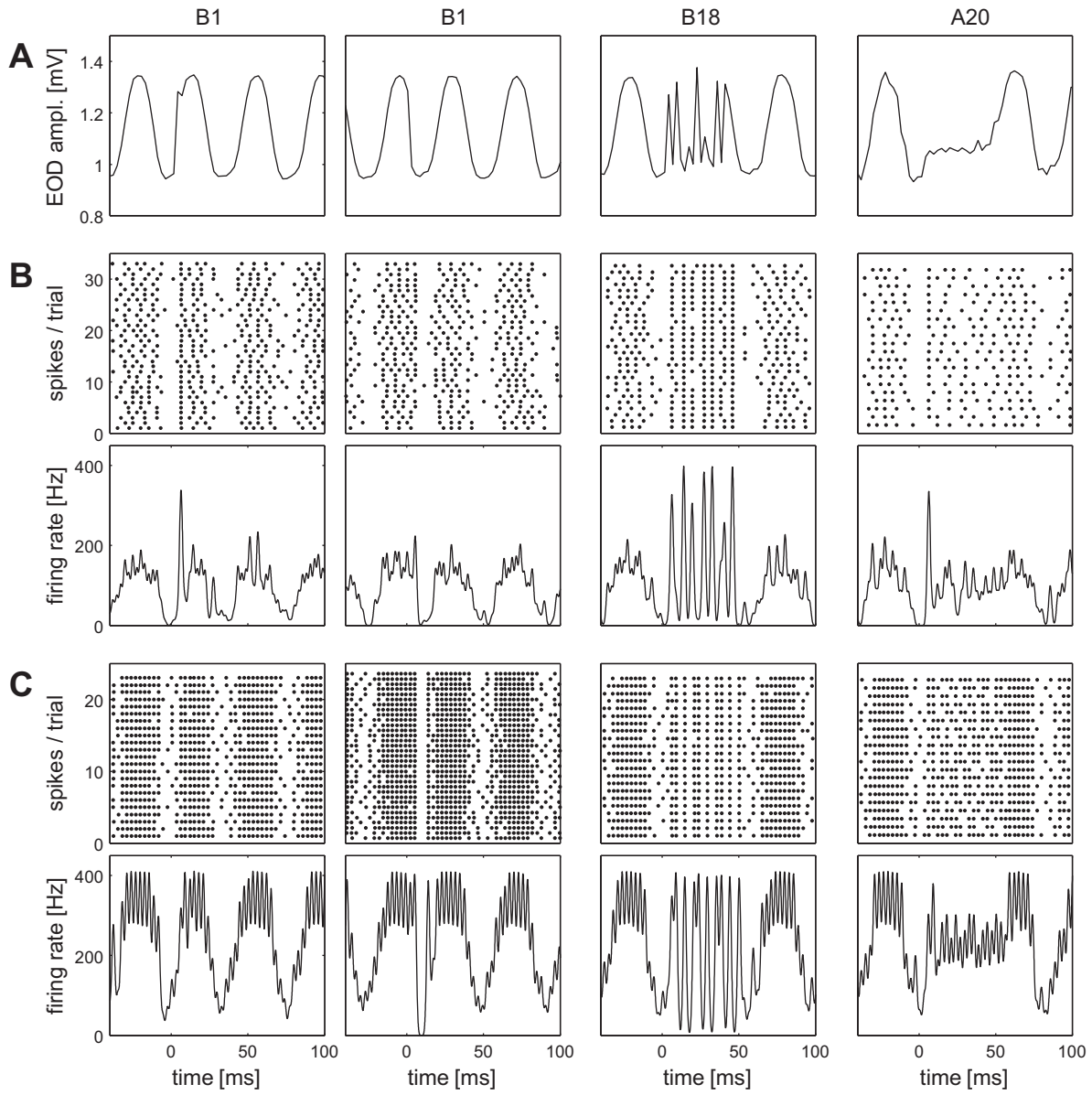

Fig. 6. Response modulations of P-units with high and low baseline rate. *A*: time courses of the AM received by the recorded fish for 4 chirp stimuli. *B*: responses of a P-unit with relatively low baseline firing rate (110 Hz, EOD rate 380 Hz). *Top*: raster plot of 33 trials. *Bottom*: PSTH. *C*: same as *B* but of a P-unit with a high baseline firing rate (240 Hz, EOD rate 340 Hz).

frequency contents (Fig. 8*B*). Moreover, the modulation of the firing rate, calculated as the firing rate derivative, was stronger during chirps than during the beat (Fig. 8*C*), as was the firing synchronicity calculated as the spike train correlation (Fig. 8*D*). For both measures, the responses were stronger for type A than type B chirps, irrespective of the strength of the low-frequency content.

Decoding Analysis

P-unit, T-units, and ampullary cells extract different features from the different chirp types. This suggests that a potential readout mechanism might benefit from the joint information contained in the different receptors for detecting and identifying these communication signals. To quantify how much information each cell type contains about each chirp type, we used a decoding approach in which we train a machine learning algorithm to distinguish between chirp and baseline responses based on the neural responses of single neurons or small populations to chirps.

We trained a SVM classifier (Boser et al. 1992; Cortes and Vapnik 1995) for each cell and each chirp type to predict whether a given trial was the mere baseline response or the response to a chirp. Baseline activity data points were randomly selected windows of activity from parts of the trials where only a beat was present, whereas chirp data points were extracted directly after the onset of the chirp. We defined the window length for each fish in terms of EOD cycles to provide a fair comparison between individuals with different EOD frequencies. SVMs were trained for window lengths of 5, 10, 20, 25, and 30 EOD cycles.

For single neurons, the SVM yielded a decision rule of the form

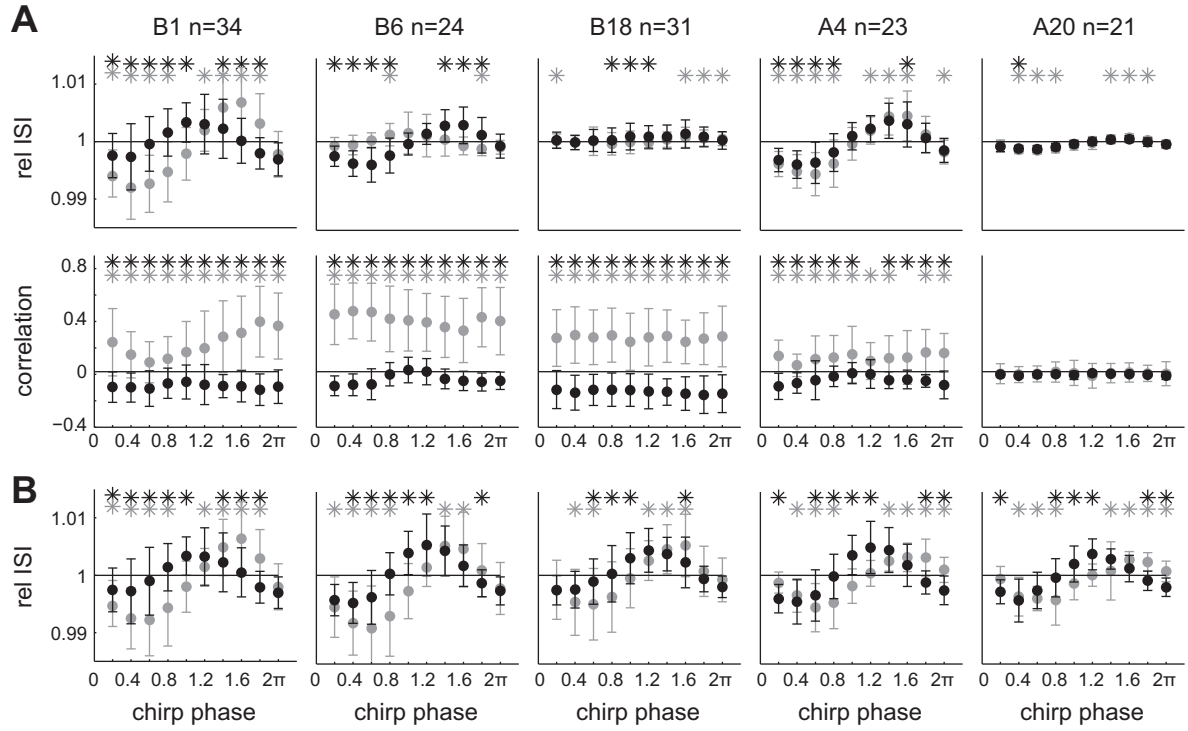

Fig. 7. T-units respond to chirps with modulations in spike timing. Averaged responses of T-units to the different chirp types (compare Fig. 2) in a 24-Hz beat. *A*: effects of chirps on the ISI (*top row*) and the ISI correlation between trials (*bottom row*) were analyzed for 10 phase relations between chirp and beat. *B*: ISIs were analyzed for the onset (1st EOD cycle) of the chirp. Error bars denote SD. Chirp response (gray) and beat response (black) were normalized to the control response (horizontal line, compare to Fig. 3). Asterisks indicate a $P < 0.01$ in a Wilcoxon signed-rank test between chirp and control response (black asterisks) as well as chirp and beat response (gray asterisks).

$$\hat{y} = \mathrm{sign}\left[\int_0^T w(t) \cdot (x * h)(t)\mathrm{d}t + b\right], \qquad (7)$$

where T is the length of the time window extracted after the chirp onset and $(x * h)(t)$ is the spike train convolved with a one-sided exponential $h(t) = [t]_+ \exp(-t/\tau)$. We use this particular filter kernel to simulate the membrane potential of a pyramidal cell postsynaptic to the receptors. $w(t)$ and b are a weighting function and an offset, respectively, which are optimized by the SVM to produce a positive response if the neural activity x results from a spike and negative if it corresponds to baseline activity. Therefore, $\hat{y}$ is the predicted label of the tested spike train x. In the following, we denote the true label with y.

We found that the weighting functions $w(t)$ were similar to the difference between the means over the convolved trials for chirp and baseline activity (Fig. *9*, *A–C*, *2nd, 3rd*, and *4th rows*). This is expected since $w(t)$ should emphasize regions in which the two conditions are most distinguishable.

As in our analyses above, neural response changes were triggered by particular features of the chirps. For instance, P-units and T-units changed their activity upon omitted EOD cycles in type B chirps (Fig. 9, *A* and *B*), whereas ampullary cells mostly responded to the long pauses of type A chirps (Fig. 9*C*). Therefore, we expected that responses of ampullary units yield more information about A-type chirps, while T-units and

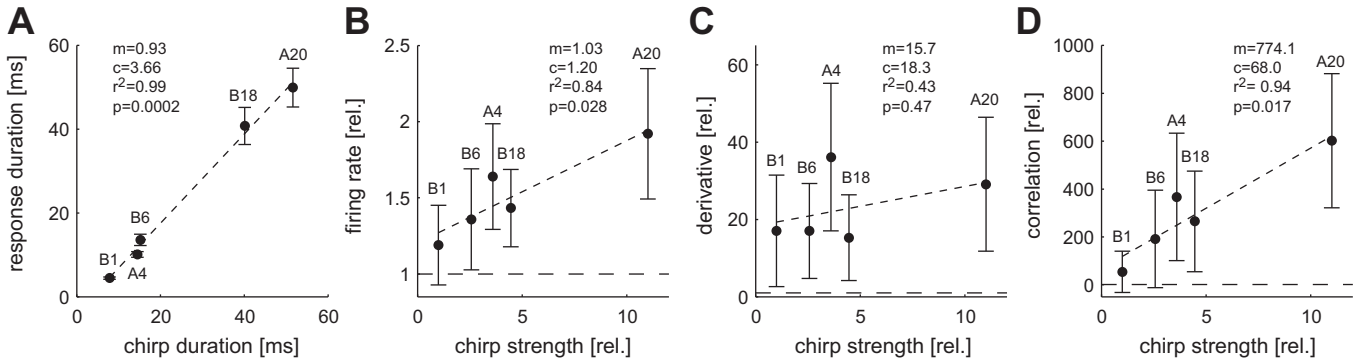

Fig. 8. Quantitative analysis of ampullary responses to chirps. The response duration (*A*) and response strength (*B*), as well as the mean derivative of the firing rate (*C*), and response correlation (*D*) of ampullary receptors were analyzed and compared with the chirp duration and chirp strength (amplitude of the low-frequency component of the chirp, normalized to the value of B1 chirps at 20% contrast), respectively. Response strength, derivative of the firing rate, and response correlation were normalized to the control firing rate, and the low-frequency component was normalized to the value of single-cycle interruptions. Dots show the mean, error bars the standard deviation. The slope (m) and the intercept (c) of the fit are indicated, as well as the correlation coefficient (r) and it's statistical evaluation according to Pearson (p). Chirp types are indicated as abbreviations (compare Fig. 3).

P-units should perform better in predicting the presence of type B chirps.

We quantified the decoding performance by the mutual information $I[Y,\hat{Y}]$ between the true and the predicted labels normalized by the maximally achievable mutual information (see METHODS). Because of the data-processing inequality (Cover and Thomas 2006), the mutual information $I[Y,\hat{Y}]$ is a lower bound on the available information about chirp vs. baseline in the neural responses (Quian Quiroga and Panzeri 2009). The mutual information was estimated for each neuron, each chirp type, and each window length from the predictions on a stratified test set consisting of 20% of the data points not used for training the SVM.

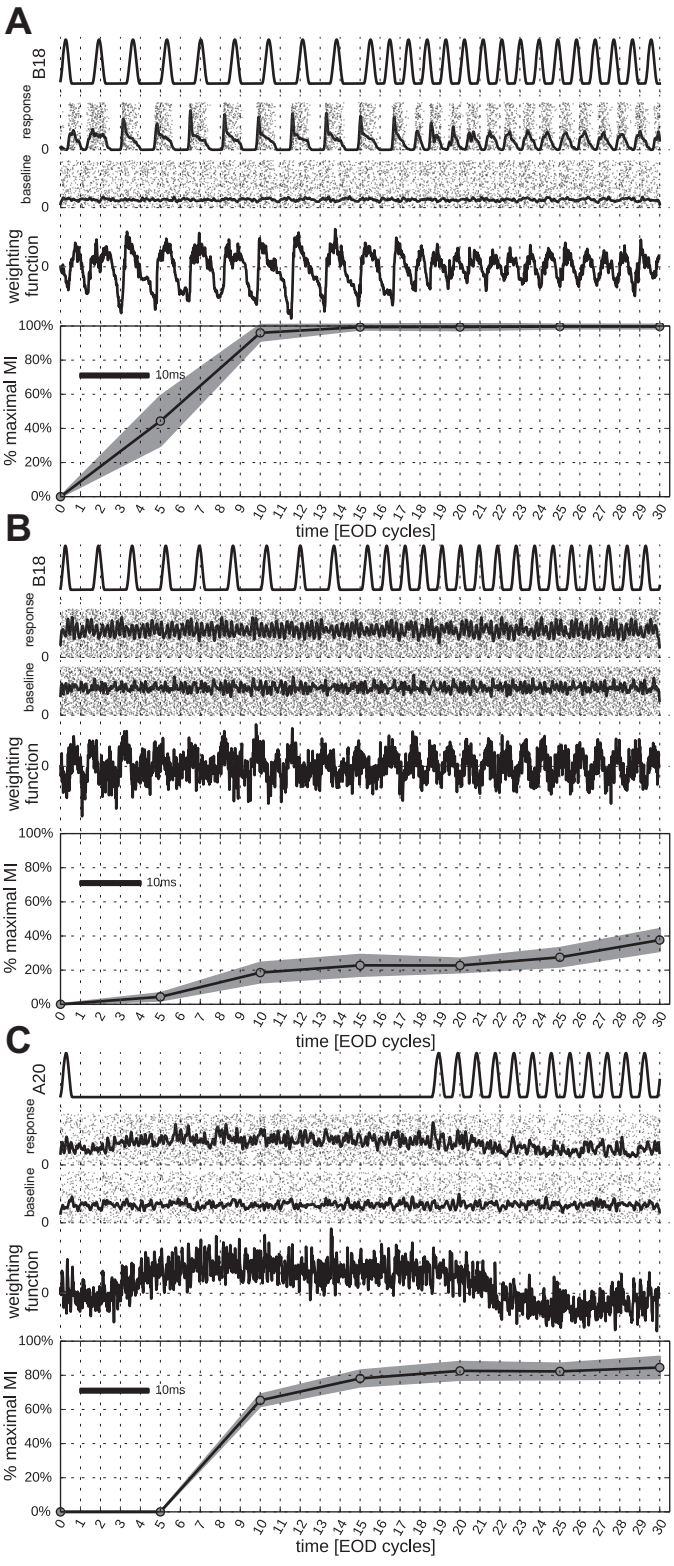

Fig. 9. Decoding of a P-unit (*A*), a T-unit (*B*), and an ampullary (*C*) receptor response to certain chirps. *Top*: stimulus, i.e., the electric field of the artificial second fish in arbitrary units. The label denotes the type of the chirp type B chirp of 18 cycles duration (B18) for the P- and T-unit and type A chirp of 20 EOD cycle duration (A20) for the ampullary receptor (note that the duration is given in relation to the chirping fish, not the receiving fish). *2nd* and *3rd rows*: responses to the chirp (*2nd row*) and a random selection to the beat alone (*3rd row*) as spike rasters and PSTH estimated as the average across trials after convolution of spikes with a Gaussian kernel ($s = 0.1$ ms). *4th row*: weighting function $w(t)$. It closely follows the difference between the baseline and the chirp PSTHs. For the responses of the P-unit and the T-unit upon a B18 chirp, the difference are most prominent after skipped EODs. For the response of the ampullary unit to a A20 chirp, the difference is strongest during the period of silence including some onset delay and a rebound response. *5th row*: decoding performance in percentage of the maximal mutual information (MI; see METHODS). Decoding performance increases with increasing trial length.

The mutual information increased with increasing number of EOD cycles available to the classifier (Fig. 9, *A–C*). For most cells, it saturated at around 15–20 EODs. Across all neurons the decoding performance was quite variable (Fig. 10), often shifting to higher percentages with increasing window lengths. P-units generally performed well on all chirp types but better on type B (Fig. 10, *1st row*). T-units also performed better on type B chirps but did not reach the same performance levels as P-units or ampullary cells (Fig. 10, *2nd row*). Ampullary units performed better on type A chirps, in particular on the long A20 chirp (Fig. 10, *3rd row*). Generally, all cells yielded the most information for longer chirps of their preferred type.

The fact that ampullary units yield more information about type A chirps while P-units and T-units perform better on type B chirps suggests that a potential readout mechanism could benefit from looking at all cell types at once. To quantify this, we assembled several populations consisting of three cells recorded from the same individual. One set of populations consisted of all cell types (Fig. 10, APT), while the other set consisted of different P-units only (Fig. 10, PPP). For populations, the decision function of the SVM (*Eq. 7*) obtained an integral term for each member cell. In the finite dimensional case, this would be equivalent to stacking the feature vectors of all neurons in the population.

Populations generally yielded more information about baseline vs. chirp responses than single units. However, except for the A20 chirp, the PPP population performed better than the mixed APT population. For the A20 chirp, the APT population yielded more information than the PPP population ($P \leq 0.006$, two independent sample *t*-test, Bonferroni corrected for five comparisons).

DISCUSSION

We investigated the neural representation of communication signals (chirps) in the parallel channels of the electrosensory system of *E. virescens*. In a first step we categorized the different communication signals recorded in behavioral experiments leading to the description of a previously undescribed

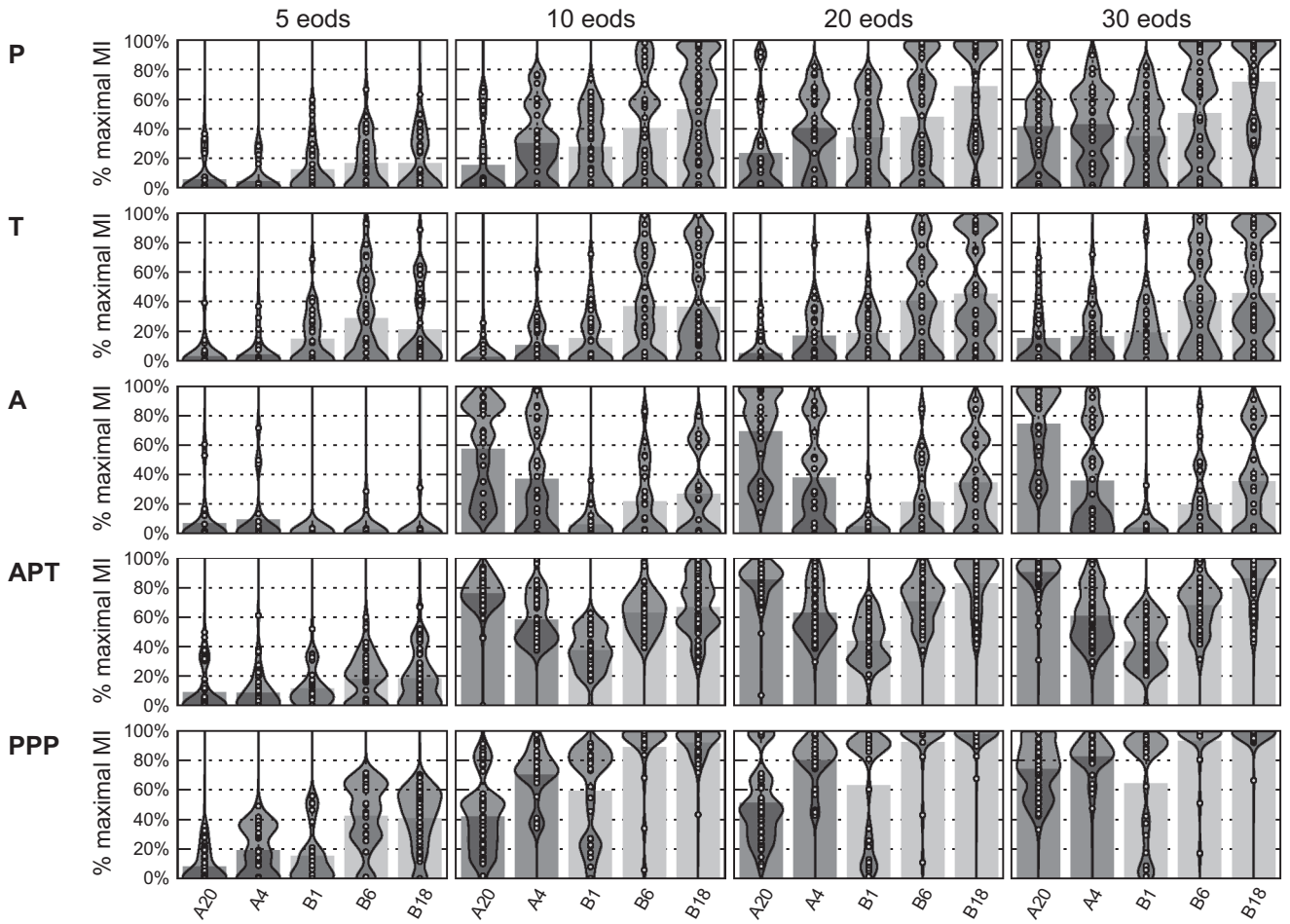

Fig. 10. Decoding performance by cell/population vs. chirp type. We report the decoding performance as mutual information between the actual label (chirp vs. baseline) and the predicted label normalized by the maximally achievable information. Letters denote the cell type or the cell types of each neuron participating in the population. Each single point denotes the average mutual information for 1 cell or population over 10 training and test sets generated by resampling. The violin plots depict the smoothed histogram. The bars denote the mean. For all cell and population types, decoding performance increases with increasing length of the time window used for classification. P-units perform well on all chirp types but better on B type (*1st row*). T-units also perform better on B-type chirps but overall worse than P-unit and ampullary cells (*2nd row*). Ampullary units perform better on A-type chirps, in particular on the long A20 chirp (*3rd row*). Populations generally perform better than single units. For all chirp types except A20, populations of 3 P-units (PPP) perform significantly better than a population of an ampullary, a P-unit, and a T-unit. For A20 chirps, the situation is reverse ($P \leq 0.006$, 2 independent sample *t*-test, Bonferroni corrected for five comparisons).

chirp type. Next, we characterized the neural representation of each chirp type in all three electroreceptor afferents and found that each type of electroreceptor extracts a distinct set of features. For P- and T-units these features were more pronounced for type B chirps while they were more distinctive for type A chirps in ampullary units. A subsequent decoding analysis on small populations of receptors suggests that a potential readout mechanism should use this complementary information of the parallel sensory channels for a reliable chirp detection.

A New Chirp Type

Eigenmannia communication signals have been described as EOD interruptions of several tens to hundreds milliseconds duration (Hopkins 1974a; Hagedorn and Heiligenberg 1985). We termed these type A chirps. In our behavioral experiments we did not observe such chirps. Rather, we recorded rapid excursions in the EOD frequency that consisted of single-cycle EOD interruptions or multiple repetitions of single-cycle interruptions that have not been described before (Fig. 1, *A–D*).

Type A chirps are closely related to mating behavior and are therefore considered social signals (Hagedorn and Heiligenberg 1985). For several reasons we believe that the type B chirps observed here can also be considered as social signals.

1) They were almost exclusively observed upon stimulation with external electric fields that mimicked conspecifics (Fig. 1*E*).

2) Qualitatively, they were similar to previously described chirps, since they were also decreases of the EOD frequency. Some of the longer chirps (Fig. 1*D*) resembled previously described "incomplete interruptions" (Hagedorn and Heiligenberg 1985). Interestingly, stimulation of the prepacemaker nucleus (PPN; Kawasaki and Heiligenberg 1988; Kawasaki et al. 1988) and the preoptic area (PEO; Wong 2000) leads to EOD modulations similar to the interruptions described in this study.

Why did we not observe long (type A) interruptions that so closely became associated with *E. virescens* communication? The main reason may be that previous observations were mostly conducted on sexually mature animals during tuberous

courtship behavior (Hagedorn and Heiligenberg 1985; Hopkins 1974a). Hopkins (1974a) shows that chirps during the breeding season are distinctly longer and are produced in higher numbers than outside the season.

It is therefore conceivable that shorter EOD interruptions are produced by *E. virescens* outside of the breeding season and possibly act as negotiation of threat signals similar to type 2 chirps in *A. leptorhynchus* (Engler and Zupanc 2001; Hupé et al. 2008), while long interruptions are produced by males in the context of courtship behavior.

Coding of Chirps in Three Types of Electroreceptors

If we assume that the different chirp types are of behavioral importance and have distinct meanings, the nervous system must be able to identify them on the basis of the electroreceptor responses. We therefore assessed how the two types of chirps are encoded in the spiking responses of the primary afferents of the three types of electroreceptors. We characterized the effects of chirps on different aspects of the neuronal responses: the firing rate (or the interspike-interval in T-units), the spike time correlation as a measure of synchronicity, and the amount of change in the firing rate.

Synchrony Is a Good Code for Chirp Types in P-Units

Single-cycle interruptions as well as short type A and B chirps lead to modulations of the P-unit firing rate around the average firing rate depending on the phase relation between beat and chirp (Fig. 4). This ambiguity renders the firing rate an inapt measure for the decoding of the neuronal responses. The level of response synchrony, however, was distinctly different between type A and type B chirps. Furthermore, the changes in response synchrony were robust against changes in the phase relation between chirps and the underlying beat. On the basis of this feature, type A chirps, on the one hand, and type B chirps and single-cycle interruptions, on the other, could be separated. This encoding scheme is surprisingly similar to a related weakly electric fish, the brown ghost knife fish, *A. leptorhynchus*. In this species, different types of chirps are encoded in P-unit synchronization and desynchronization as well (Benda et al. 2006; Walz et al. 2014), despite the very different nature of the communication signals that are transient increases in EOD frequency and do not contain low-frequency components.

The responses of P-units of *E. virescens* were qualitatively similar for slow and fast beats (compare Figs. 4 and 5), as well as for negative beats. In *A. leptorhynchus*, however, chirps can have opposing effects on P-unit responses, depending on the beat frequency (Benda et al. 2006; Hupé et al. 2008; Walz et al. 2014). In this species, sexual dimorphism in EOD frequency is very pronounced and EOD frequency is correlated with sex (Dunlap et al. 1998). Therefore, beats in intersexual encounters are likely of the same sign. In *E. virescens*, however, there is only a statistical correlation between sex and EOD frequency (males tend to have lower frequencies than females), and this is most pronounced in sexually mature animals (Hopkins 1974a). Recordings show that males that chirp vigorously during courtship behavior could even have higher EOD frequencies than their accompanying females (Fig. 7 in Hopkins 1974a and Fig. 5 in Hagedorn and Heiligenberg 1985). It is therefore likely that chirps often occur in beats of different signs and thus an encoding scheme that is largely independent of the beat appears appropriate in *E. virescens*.

T-Units Can Encode Chirp Features in their Spike Timing

T-units are driven by the fish's own EOD and fire one spike to each discharge of the electric organ. They encode the phase of the beat in their spike timing, which can be compared across different body areas and the phase modulations can be extracted (Bastian and Heiligenberg 1980; Rose and Heiligenberg 1986; Lytton 1991; Fortune et al. 2006). T-units have been shown to respond to self-generated chirps by ceasing to fire during the interruptions because there was no EOD present (Metzner and Heiligenberg 1991). We give the first account of T-units responding to chirps in a receiving fish. Since the receiver's EOD was still present, T-units continuously fired action potentials during the chirps (Fig. 3*B*) and the firing rate therefore is uninformative. However, chirps generated modulations of ISIs (Fig. 3*B*). Type B chirps generated the strongest ISI modulations while type A chirps were only marked by brief changes in the ISI mostly at the beginning. Similar to P-units, these ISI modulations were strongly correlated across trials especially upon type B but not type A chirps (Fig. 7). Reading out the modulation of the ISIs of T-units may thus support the discrimination between type A and type B chirps.

Ampullary Responses Encode the Duration of Chirps

The firing rate and response synchrony of ampullary receptors increased in response to all types of chirps compared with the control. This is in accordance with observations on ampullary responses to self-generated chirps (Metzner and Heiligenberg 1991). The response strength was correlated to the amount of low-frequency content (Figs. 3 and 8*B*). However, the response to short type A chirps was stronger than to long type B chirps, even though the latter had a stronger absolute low-frequency component. We found the same pattern for the derivative of the firing rate, as well as the firing synchrony (Fig. 8, *C* and *D*). Therefore, it is hard to conceive how ampullary receptors could encode the chirp type in the modulation of their firing rate. Moreover, the strength of low-frequency content does not only depend on the type of chirp but also on how close the chirping fish is to the receiver, which makes encoding of chirp types via the firing rate even more ambiguous. Ampullary receptors could, however, encode the duration of a chirp in the duration of their response (Fig. 8*A*). Thus, while it is not possible to discern chirp types unambiguously from ampullary responses, the occurrence and duration of the chirp are reliably encoded.

Decoding of Eigenmannia Communication Signals

It is likely that the different chirp types have different behavioral meanings in social encounters of the fish. Therefore, reliably distinguishing these communication signals is crucial perceptual task for the animal. Our results show that communication signals are encoded by all three types of electroreceptors. Chirps can consist of combinations of longer and shorter interruptions (Fig. 1*D*) which cause characteristic response profiles in each receptor type (Fig. 3).

Depending on the chirp type certain receptors are better suited to detect certain their presence than others (Fig. 10, A, P, T). The most prominent feature of long type A chirps,

the putative courtship signals, is their strong low-frequency component, which causes little firing rate modulation and desynchronization in P-and T-units but strong increases in firing rate and synchronization in ampullary receptors. Type B chirps, possible negotiation signals, on the other hand, are characterized by strong firing rate modulation and synchronization in P-units and T-units, while the weaker low-frequency component induces less pronounced changes in ampullary responses. Our single-unit decoding analysis confirms that type B chirps are better detected in P- and T- units while ampullary response provide more information about type A chirps (Fig. 10, A, P, T).

However, any chirp contains features that drive both the tuberous and the ampullary system at the same time. This suggests that a potential readout mechanism could benefit from combining information from all electroreceptor types in at least two ways: both systems are subjected to environmental noise from various sources (Metzner and Heiligenberg 1991; Benda et al. 2013), and integration of the tuberous and the ampullary system could improve the robustness of detection. Moreover, combining information from different receptor types could reduce ambiguities. The population decoding analysis (Fig. 10, APT, PPP) demonstrates that chirps can be detected more faithfully from the response of several receptors. For most chirp types, detection performance based on P-units activity alone turned out to be superior to that of the single-unit or mixed population. Chirps with long interruptions, however, are more reliably decoded by mixed populations of the tuberous and ampullary receptors. However, type A chirps have been reported with durations in the range from 100 ms up to 2 s (Hopkins 1974b; Hagedorn and Heiligenberg 1985), which is considerably larger than the longest type A chirp we used (A 20). Therefore, the fact that it is only this chirp that is more reliably detected by the mixed population could simply be a consequence of the limited stimulus set, which would mean that our analysis rather underestimates the importance of parallel processing in tuberous and ampullary system. We therefore conclude from our results that the type B negotiation signals could be well decoded on the basis of P-units alone, while the detection of courtship signals (type A chirps) clearly profits from combining ampullary and P-unit responses. Combining information from these parallel channels can reduce ambiguity in the signals, and make encoding more robust.

ACKNOWLEDGMENTS

We thank Rüdiger Krahe for help establishing *Eigenmannia* recordings in our laboratory, and Henriette Walz and Janez Prešern for comments and discussion.

GRANTS

J. Benda and J. Grewe are supported by Bundesministerium für Bildung und Forschung (BMBF) Grant 01GQ0802. F. Sinz is partly funded by Bernstein Center for Computational Neuroscience Tübingen (BMBF Grant 01GQ1002).

DISCLOSURES

No conflicts of interest, financial or otherwise, are declared by the author(s).

AUTHOR CONTRIBUTIONS

Author contributions: A.S., J.B., and J.G. conception and design of research; A.S. and J.G. performed experiments; A.S., F.S., and J.G. analyzed data; A.S., J.B., and J.G. interpreted results of experiments; A.S. prepared figures; A.S. drafted manuscript; A.S., F.S., J.B., and J.G. edited and revised manuscript; A.S., F.S., J.B., and J.G. approved final version of manuscript.

REFERENCES

Bastian J, Heiligenberg W. Neural correlates of the jamming avoidance response of *Eigenmannia*. *J Comp Physiol A* 136: 135–152, 1980.

Bastian J, Schniederjan S, Nguyenkim J. Arginine vasotocin modulates a sexually dimorphic communication behavior in the weakly electric fish Apteronotus leptorhynchus. *J Exp Biol* 204: 1909–1923, 2001.

Benda J, Grewe J, Krahe R. Neural noise in electrocommunication: from burden to benefits. In: *Animal Communication and Noise*, edited by Brumm H. Berlin, Germany: Springer, vol 2, 2013, p. 331–372.

Benda J, Longtin A, Maler L. Spike-frequency adaptation separates transient communication signals from background oscillations. *J Neurosci* 25: 2312–2321, 2005.

Benda J, Longtin A, Maler L. A synchronization-desynchronization code for natural communication signals. *Neuron* 52: 347–358, 2006.

Bensmaia SJ. Tactile intensity and population codes. *Behav Brain Res* 190: 165–173, 2008.

Boser BE, Guyon IM, Vapnik VN. A training algorithm for optimal margin classifiers. In: *Proceedings of the 5th Annual ACM Workshop on Computational Learning Theory*, 1992, p. 144–152.

Bullock T, Hamstra R, ScheichH. The jamming avoidance response of high frequency electric fish. *J Comp Physiol A* 77: 1–22, 1972.

Bullock TH, Chichibu S. Further analysis of sensory coding in electroreceptors of electric fish. *Proc Natl Acad Sci USA* 54: 422–429, 1965.

Cortes C, Vapnik V. Support-vector networks. *Machine Learning* 20: 273–297, 1995.

Cover TM, Thomas JA. *Elements of Information Theory* (2nd ed, *Wiley Series in Telecommunications and Signal Processing*). New York: Wiley-Interscience, 2006.

Duda RO Hart PE, Stork DG. *Pattern Classification* (2nd ed). New York: Wiley-Interscience, 2000.

Dunlap KD, Oliveri LM. Retreat site selection and social organization in captive electric fish, *Apteronotus leptorhynchus*. *J Comp Physiol A Neuroethol Sens Neural Behav Physiol* 188: 469–477, 2002.

Dunlap KD, Thomas P, Zakon HH. Diversity of sexual dimorphism in electrocommunication signals and its androgen regulation in a genus of electric fish, *Apteronotus*. *J Comp Physiol A* 183: 77–86, 1998.

Dye J. Dynamics and stimulus-dependence of pacemaker control during behavioral modulations in the weakly electric fish, *Apteronotus*. *J Comp Physiol A* 161: 175–185, 1987.

Engler Z and Zupanc GK. Differential production of chirping behavior evoked by electrical stimulation of the weakly electric fish, *Apteronotus leptorhynchus*. *J Comp Physiol A* 187: 747–756, 2001.

Fortune ES, Rose GJ, Kawasaki M. Encoding and processing biologically relevant temporal information in electrosensory systems. *J Comp Physiol A* 192: 625–635, 2006.

Hagedorn M, Heiligenberg W. Court and spark: electric signals in the courtship and mating of gymnotoid fish. *Anim Behav* 33: 254–265, 1985.

Heiligenberg W. The jamming avoidance response in the weakly electric fish *Eigenmannia*. A behavior controlled by distributed evaluation of electroreceptive afferences. *Naturwissenschaften* 67: 499–507, 1980.

Heiligenberg W. *Neural Nets in Electric Fish*. Cambridge, MA: MIT Press, 1991.

Hopkins CD. Electric communication: functions in the social behavior of Eigenmannia virescens. *Behaviour* 50: 270–305, 1974a.

Hopkins CD. Electric communication in the reproductive behavior of *Sternopygus macrurus* (Gymnotoidei). *Z Tierpsychol* 35: 518–535, 1974b.

Hopkins CD. Stimulus filtering and electroreception: tuberous electroreceptors in three species of Gymnotoid fish. *J Comp Physiol A* 111: 171–207, 1976.

Hunter JD. Matplotlib: a 2D graphics environment. *Comput Sci Eng* 9: 90–95, 2007.

Hupé GJ, Lewis JE, Benda J. The effect of difference frequency on electrocommunication: chirp production and encoding in a species of weakly electric fish, *Apteronotus leptorhynchus*. *J Physiol (Paris)* 102: 164–172, 2008.

Kawasaki M, Heiligenbergn W. Individual prepacemaker neurons can modulate the pacemaker cycle of the gymnotiform electric fish, *Eigenmannia*. *J Comp Physiol A* 162: 13–21, 1988.

Kawasaki M, Maler L, Rose GJ, Heiligenbergn W. Anatomical and functional organization of the prepacemaker nucleus in gymnotiform electric fish: the accommodation of two behaviors in one nucleus. *J Comp Neurol* 276: 113–131, 1988.

Kramer B. The sexually dimorphic jamming avoidance response in the electric fish *Eigenmannia* (Teleostei, Gymnotiformes). *J Exp Biol* 130: 39–62, 1987.

Lytton WW. Simulations of a phase comparing neuron of the electric fish *Eigenmannia*. *J Comp Physiol A* 169: 117–125, 1991.

Marsat G, Maler L. Neural heterogeneity and efficient population codes for communication signals. *J Neurophysiol* 104: 2543–2555, 2010.

Metzner W, Heiligenberg W. The coding of signals in the electric communication of the gymnotiform fish *Eigenmannia*: from electroreceptors to neurons in the torus semicircularis of the midbrain. *J Comp Physiol A* 169: 135–150, 1991.

Nassi JJ, Callaway EM. Parallel processing strategies of the primate visual system. *Nat Rev Neurosci* 10: 360–372, 2009.

Park IM, Seth S, Li L, Principe JC. Kernel methods on spike train space for neuroscience: a tutorial. *Signal Process Mag IEEE* 30: 149–160, 2013.

Pedregosa F, Varoquaux G, Gramfort A, Michel V, Thirion B, Grisel O, Blondel M, Prettenhofer P, Weiss R, Dubourg V, Vanderplas J, Passos A, Cournapeau D, Brucher M, Perrot M, Duchesnay E. Scikit-learn: machine learning in Python. *J Machine Learning Res* 12: 2825–2830, 2011.

Quian Quiroga R, Panzeri S. Extracting information from neuronal populations: information theory and decoding approaches. *Nat Rev Neurosci* 10: 173–185, 2009.

Rose G, Heiligenberg W. Neural coding of difference frequencies in the midbrain of the electric fish *Eigenmannia*: reading the sense of rotation in an amplitude-phase plane. *J Comp Physiol A* 158: 613–624, 1986.

Scheich H, Bullock TH, Hamstra R Jr. Coding properties of two classes of afferent nerve fibers: high-frequency electroreceptors in the electric fish, *Eigenmannia*. *J Neurophysiol* 36: 39–60, 1973.

Schölkopf B, Smola AJ. *Learning with Kernels: Support Vector Machines, Regularization, Optimization, and Beyond (Adaptive Computation and Machine Learning)*. Cambridge, MA: MIT Press, 2002.

Tan EW, Nizar JM, Carrera-GE, Fortune ES. Electrosensory interference in naturally occurring aggregates of a species of weakly electric fish, *Eigenmannia virescens*. *Behav Brain Res* 164: 83–92, 2005.

Todd BS, Andrews DC. The identification of peaks in physiological signals. *Comput Biomed Res* 32: 322–335, 1999.

Vonderschen K, Chacron MJ. Sparse and dense coding of natural stimuli by distinct midbrain neuron subpopulations in weakly electric fish. *J Neurophysiol* 106: 3102–3118, 2011.

Walz H, Grewe J, Benda J. Static frequency tuning accounts for changes in neural synchrony evoked by transient communication signals. *J Neurophysiol* 112: 752–765, 2014.

Wässle H. Parallel processing in the mammalian retina. *Nat Rev Neurosci* 5: 747–757, 2004.

Watanabe A, Takeda K. The change of discharge frequency by ac stimulus in a weak electric fish. *J Exp Biol* 40: 57–66, 1963.

Wong CJ. Electrical stimulation of the preoptic area in *Eigenmannia*: evoked interruptions in the electric organ discharge. *J Comp Physiol A* 186: 81–93, 2000.

Zakon H. The electroreceptive periphery. In: *Electroreception*, edited by Bullock T, Heiligenberg W. New York: John Wiley & Sons, 1986, p. 103–156.

Zakon HH, Dunlap KD. Sex steroids and communication signals in electric fish: a tale of two species. *Brain Behav Evol* 54: 61–69, 1999.

Zakon HH, Thomas P, Yan HY. Electric organ discharge frequency and plasma sex steroid levels during gonadal recrudescence in a natural population of the weakly electric fish *Sternopygus macrurus*. *J Comp Physiol A* 169: 493–499, 1991.